

See discussions, stats, and author profiles for this publication at: <https://www.researchgate.net/publication/5241737>

Hydrogen Bond Breaking Mechanism and Water Reorientational Dynamics in the Hydration Layer of Lysozyme

Article in *The Journal of Physical Chemistry B* · August 2008

DOI: 10.1021/jp800998w · Source: PubMed

CITATIONS

52

READS

207

3 authors, including:



Biman Jana

Indian Association for the Cultivation of Science

95 PUBLICATIONS 1,801 CITATIONS

[SEE PROFILE](#)



Biman Bagchi

Indian Institute of Science

571 PUBLICATIONS 18,811 CITATIONS

[SEE PROFILE](#)

Some of the authors of this publication are also working on these related projects:



Effect of Fluorination on the Photophysics of Biologically Relevant Molecules [View project](#)



Chemical denaturation, Protein folding/unfolding [View project](#)

Hydrogen Bond Breaking Mechanism and Water Reorientational Dynamics in the Hydration Layer of Lysozyme

Biman Jana, Subrata Pal, and Biman Bagchi*

Solid State and Structural Chemistry Unit, Indian Institute of Science, Bangalore 560 012, India

Received: February 2, 2008; Revised Manuscript Received: April 17, 2008

The mechanism and the rate of hydrogen bond-breaking in the hydration layer surrounding an aqueous protein are important ingredients required to understand the various aspects of protein dynamics, its function, and stability. Here, we use computer simulation and a time correlation function technique to understand these aspects in the hydration layer of lysozyme. Water molecules in the layer are found to exhibit three distinct bond-breaking mechanisms. A large angle orientational jump of the donor water molecule is common among all of them. In the most common ($\approx 80\%$) bond-breaking event in the layer, the new acceptor water molecule comes from the first coordination shell (initially within 3.5 Å of the donor), and the old acceptor water molecule remains within the first coordination shell, even after the bond-breaking. This is in contrast to that in bulk water, in which both of the acceptor molecules involve the second coordination shell. Additionally, the motion of the incoming and the outgoing acceptor molecules involved is not diffusive in the hydration layer, in contrast to their observed diffusive motion in the bulk. The difference in rotational dynamics between the bulk and the hydration layer water molecules is clearly manifested in the calculated time-dependent angular van Hove self-correlation function ($G(\theta, t)$) which has a pronounced two-peak structure in the layer, and this can be traced to the constrained translational motion in the layer. The longevity of the surrounding hydrogen bond network is found to be significantly enhanced near a hydrophilic residue.

I. Introduction

Water molecules in the hydration layer of biomolecules, sometimes referred to as “biological water”, not only are important for the thermodynamic stability of the proteins and DNA, but also play a central role in several biomolecular functionalities, such as intercalation, catalysis, recognition, etc.^{1–7} Because of their extended hydrogen bond network, water molecules in the bulk liquid state are well-known to exhibit a myriad of anomalous properties, which are beginning to be understood.^{8,9} These properties can become even more anomalous in the hydration layer of biomolecules that offer a complex, charged, heterogeneous surface.^{9–13} Naturally, the dynamics of water in the hydration layer exhibits a considerably different behavior as compared to its bulk state. In particular, the translational and the rotational dynamics of water in the hydration layer are slower than those in the bulk water.⁴ Several recent studies have examined the consequence of the disruption of the extended hydrogen bond network of water at the protein surface.^{11–15} Although a few water molecules can form strong hydrogen bonds with the polar amino acid residues, many water molecules at the surface are not hydrogen bonded to any of the amino acid residues. However, water can still form a quasi-two-dimensional connected hydrogen bond (HB) network/cluster around the protein surface.¹⁴ Because of the presence of the protein surface, the nature of this HB network around the protein is different from that in the bulk. Recently, the hydration structure of human lysozyme was analyzed by using molecular dynamics simulations.¹⁵ It was found that the network is particularly stable near the hydrophilic patches, thus reflecting

the role of electrostatic interaction between the polar amino acid residues and the water molecule in stabilizing the hydrogen bond network.¹⁵

The microscopic aspects of hydrogen bond breaking and water reorientation in the bulk and in the hydration layer of an anion have been examined recently by Laage and Hynes.^{16–18} It was found that to reorient significantly, the HB donor water molecule must break the H-bond involving the rotating hydrogen. In a hydrogen bond-breaking event, the H-bond migrates from one acceptor water molecule to another. It was found that such a hydrogen bond-switching event (HBSE) is rather complex, with the new acceptor water molecule entering the fray from the second coordination shell and creating a five-coordinated transition state of the donor molecule.^{16,17,19} After HBSE, the old acceptor leaves the scene and goes out to the second coordination shell. Across a HBSE, the reorientation occurs via a large angle jump (about 60°) of the rotating O–H bond.^{16,17} Such an examination of water reorientation in the hydration layer of a protein surface is still missing.

In this article, we present the important mechanistic and dynamical features of the HBSEs in the hydration layer of a lysozyme and compare the same with the bulk water. We discuss the longevity of the connected network/cluster of water in the hydration layer. We show that the results bring out the important role of translation–rotation coupling in the rotational dynamics of water molecules in the bulk and the hydration layer.

II. Methods

Lysozyme. Lysozyme is a globular protein with 129 amino acids, of which 69 amino acids are hydrophilic and other 60 amino acids are hydrophobic. In its solvated state, many of the water molecules in the hydration layer are H-bonded to the polar groups of the amino acid residues and the backbone. At the

* Corresponding author. E-mail: bbagchi@sscu.iisc.ernet.in.

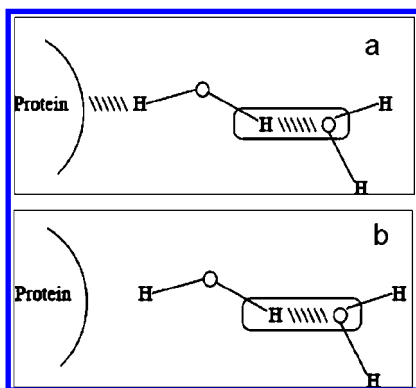


Figure 1. Schematic representation of the WW hydrogen bonds in the hydration layer of lysozyme with (a) donor bound to protein polar groups (hydrophilic residue), and (b) free donor (near hydrophobic residue).

same time, many more of the water molecules in the hydration layer are not hydrogen bonded to the protein, especially when they are near the hydrophobic residues. On an average, $\sim 30\%$ of the total water molecules in the hydration layer of lysozyme are H-bonded to the protein (with the polar group of backbone and side chains).

Molecular Dynamics Simulation. We have carried out classical molecular dynamics simulations using the well-known GROMACS package.²⁰ We have used the SPC/E model for water molecules.²¹ The trajectory of the bulk water was propagated using a leapfrog integrator with a time step of 0.5 fs. We have employed the periodic boundary condition, and the long-range Coulombic interactions were calculated using Ewald summation.²² The bulk water system (481 water molecules) was equilibrated for 50 ps at 300 K in canonical ensemble, and then the trajectory was propagated in a micro-canonical ensemble for 100 ps. For the simulation at 250 K, we have equilibrated the system in a NPT ensemble, and the trajectory was propagated in a microcanonical ensemble for 2 ns. For the lysozyme–water system (lysozyme in 5995 SPC/E water), we have equilibrated the system in a NPT ensemble at 300 K, and the trajectory was propagated in a NVT ensemble.

Selection of Hydration Layer Water. We have selected the water molecule as the hydration layer water if it resides within 4.25 Å of any of the heavy atoms of the protein, on the basis of the radial distribution function calculated for water molecules in the system with respect to the protein atoms.

Definition of the OH \cdots O H-Bond. To detect the H-bond switching events along a molecular dynamics trajectory, criteria for the existence of the H-bond have to be chosen. We have chosen the widely used geometric definition:^{23–26} $D_{O^* \cdots O^n} < 3.5$ Å, $\theta_{HO^*O} < 30^\circ$, where $D_{O^* \cdots O^n}$ is the distance between the donor and the acceptor oxygen atoms, and θ_{HO^*O} is the angle between the O–H bond and the OO vectors.

Characteristic Geometrical Parameters of a HBSE. The H-bond donor water molecule is designated as HO $^*H^*$ where O $^*H^*$ is the rotating bond. The old acceptor molecule that breaks the H-bond with H * is represented as O oH_2 , and the new acceptor molecule is represented as O nH_2 . We monitor oxygen–oxygen distances $D_{O^* \cdots O^o}$ and $D_{O^* \cdots O^n}$, together with the angle θ between the projection of O $^*H^*$ vector on the O $^oO^*O^n$ plane and the O $^oO^*O^n$ angle bisector (for detailed information, see Figure 2 of ref 16). $\theta = 0^\circ$, when H * is equidistant from both O o and O n , characterizes the HBSE.

III. Results and Discussions

(A) Mechanism of HB Breaking. We first categorize the two types of water–water (WW) hydrogen bonds present in the hydration layer of lysozyme. Figures 1a and b display a schematic representation of WW hydrogen bonds for the bound (by HB to protein) and free donor, respectively. Hydrogen bonds with bound water (BDHB) are found near the hydrophilic residues of the protein, whereas hydrogen bonds with a free donor (FDHB) are found near the hydrophobic residues. We next discuss the mechanism of the WW hydrogen bonds in the hydration layer and compare the same with that in the bulk water. Detailed descriptions of the characteristic geometrical parameters used for the mechanistic characterization of the HBSEs are presented in the Methods section.

Note that the three important characteristics that are common for almost all of the HBSEs in bulk water are (i) a jump ($\sim 60^\circ$) in the angular direction of the rotating O $^*H^*$ bond across the HBSE and (ii) the new acceptor molecule, O nH_2 , comes from the second coordination shell ($D_{O^* \cdots O^n} > 4.1$ Å) to the first coordination shell ($D_{O^* \cdots O^n} < 3.5$ Å) of the donor water (O *H_2) and (iii) the old acceptor molecule, O oH_2 , goes out from the first coordination shell to the second coordination shell of the donor water diffusively. Figure 2a shows the evolution of $D_{O^* \cdots O^o}$ and $D_{O^* \cdots O^n}$ (lower panel) and θ (upper panel) before and after a HBSE event in the bulk water.

Now we discuss HBSE in the hydration layer. We have identified and analyzed 800 water–water (WW) HBSEs, all in the layer. The mechanisms of reorientation of the water molecule in the hydration layer have been characterized by following the method developed recently.¹⁶ On the basis of the evolution of O \cdots O distances before and after the bond-breaking event, these events can be divided into three categories:

(i) Both of the acceptor molecules are initially within the first coordination shell of the donor before HBSE and remain there even after the HBSE. This mechanism is the most prevalent ($\approx 80\%$ of all the HBSEs) in the hydration layer. This mechanism is clearly a consequence of the two-dimensional network of water around the protein surface. Figure 2b shows a representative sample of the evolution of $D_{O^* \cdots O^o}$ and $D_{O^* \cdots O^n}$ (lower panel) and θ (upper panel) before and after (1 ps) a HBSE of this type of mechanism. Note that the motion of the incoming and the outgoing acceptor molecules are not diffusive prior to and even after the H-bond-breaking event. We find a sharp jump in the angular direction of the rotating O $^*H^*$ bond across the HBSE of this mechanism (see the upper panel of Figure 2b).

The constrained motion of the old acceptor, which is not allowed to go out from the first coordination shell of the donor, after the H-bond-breaking bears the signature of the presence of a connected network of water at the lysozyme surface.^{14,15} If the old acceptor were to go out from the first coordination shell to the second coordination shell of the donor, connectivity would need to be rearranged, which is both energetically and entropically demanding. Similarly, the network prevents the new acceptor molecule from entering from the second coordination shell.

(ii) In the second type of mechanism (present in $\approx 10\%$ of all HBSEs), the new acceptor molecule (O nH_2) comes from the second coordination shell to the first coordination shell of the donor. However, the old acceptor molecule (O oH_2) remains in the hydration shell before and even after the HBSE and does not leave from the first coordination shell of the donor after the breaking event. Figure 2c shows the evolution of $D_{O^* \cdots O^o}$, $D_{O^* \cdots O^n}$ (lower panel) and θ (upper panel) before and after a HBSE of this type of mechanism. Although the left-hand part

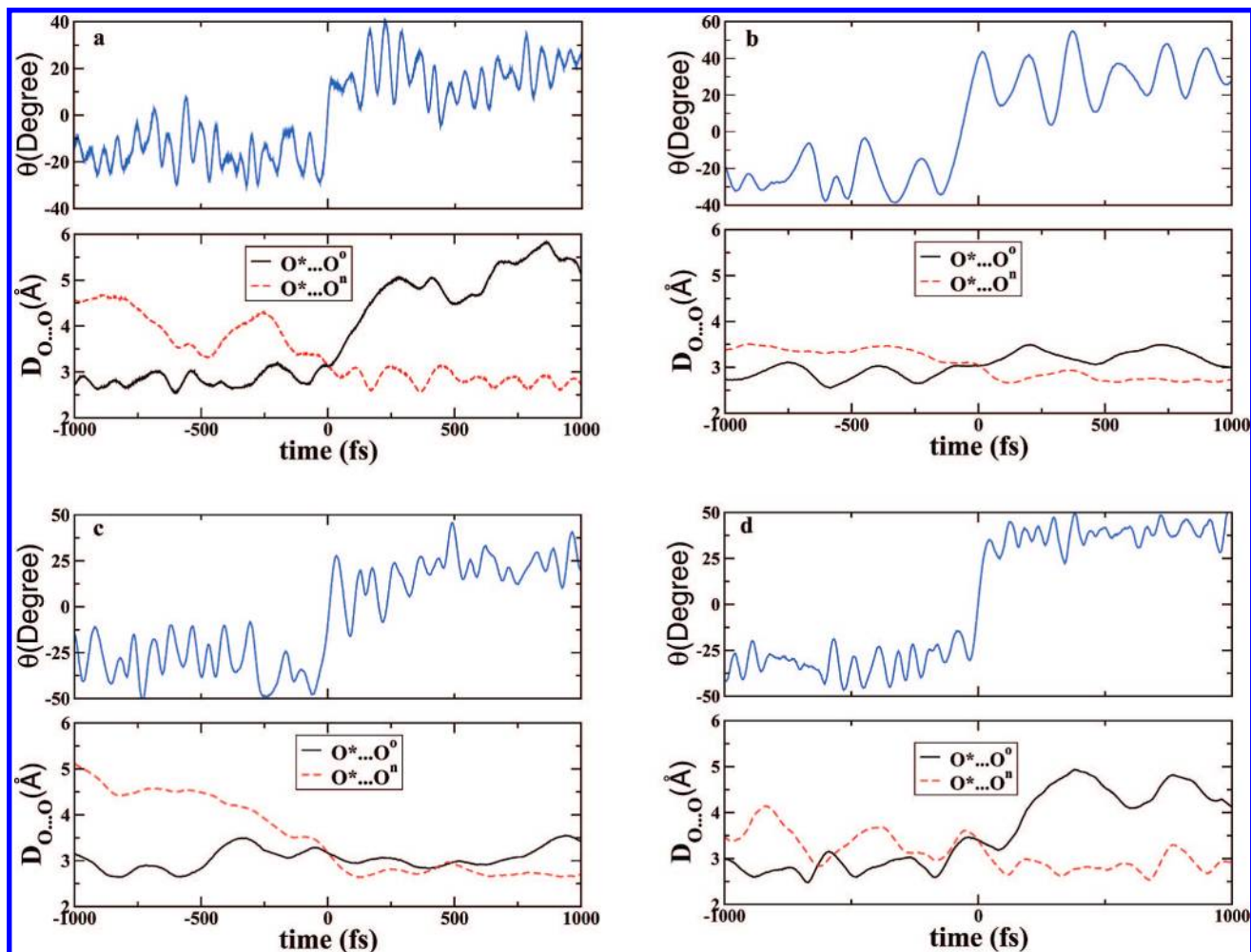


Figure 2. (a) The evolution of the characteristic parameters ($D_{O^*...O^o}$, $D_{O^*...O^n}$, and θ) across the HBSE in bulk water. The lower panel displays the evolution of the distances between the acceptor (O^oH_2 is the old acceptor molecule, and O^*H_2 is the new acceptor molecule) and the donor (O^*H_2) water molecules across the switch. The upper panel shows the evolution of the angular direction of the rotating O^*-H^* bond across the switch. Note the diffusive nature of the water molecules and large angle jump here. (b) The evolution of the characteristic parameters across the HBSE of the first mechanism in the hydration layer. For a detailed description of the upper and lower panels, see the caption of panel a. Note the constrained translational motion on both sides of the switch and the large angle jump. (c) The evolution of the characteristic parameters across the HBSE of the second mechanism in the hydration layer. For a detailed description of the upper and lower panels, see the caption of panel a. Note the constrained translational motion in the right side of the switch and the large angle jump. (d) The evolution of the characteristic parameters across the HBSE of the third mechanism in the hydration layer. For a detailed description of the upper and lower panels, see the caption of panel a. Note the constrained translational motion in the left side of the switch and the large angle jump.

(before the breaking event) of the lower panel of Figure 2c is characteristically the same as the lower panel of Figure 2a, the right-hand part (after the breaking event) is different. We again find a large angular jump (see the upper panel of Figure 2c) for the donor water molecules across the HBSE.

(iii) In the third kind of mechanism (present in $\approx 10\%$ of all HBSEs), both of the acceptor molecules are initially in the first coordination shell of the donor, but finally, the old acceptor moves out of the first coordination shell after the bond-breaking. The evolution of the characteristic parameters across a HBSE of this type of mechanism is displayed in Figure 2d. Although the right-hand part (after the breaking event) of the lower panel of Figure 2d is characteristically the same as the lower panel of Figure 2a, the left-hand part (before the breaking event) is different. The left-hand part of this mechanism provides the signature of the lower mobility of water molecules inside the hydration layer. Here also we find a sharp change in the angular direction of the rotating O^*-H^* bond across the HBSE.

We should mention that there exist several aspects^{16,17} that are common among the three mechanisms along with the

mechanism in bulk water presented here, and they are as follows: (1) the large angular jump of the rotating O^*-H^* bond across the HBSE, (2) an increase in the coordination number of the old acceptor molecule and a decrease in the coordination number of the new acceptor molecule before the HBSE, and (3) an increase in the number of H-bonds accepted by O^o and a decrease in the number of H-bonds accepted by O^n before the HBSE. However, despite the above-mentioned similarities, the mechanisms are different from each other in the evolution of the $O^o...O$ distances between the participant acceptor and the donor molecules prior to and after the bond-breaking event (lower panels of Figure 2a–d). Another important observation is that the first mechanism is found to be operative more near the hydrophilic residue, and the second and third mechanisms are found to be more operative near the hydrophobic residue.

(B) Kinetics of HB Breaking. We have calculated the average forward rate of all WW HBSEs in the hydration layer and compared the same with that in the bulk water. To this end, we have calculated the correlation function ($1 - \langle n_a(0) n_b(t) \rangle$), where n_a is 1 when H^* is hydrogen-bonded to O^o and 0

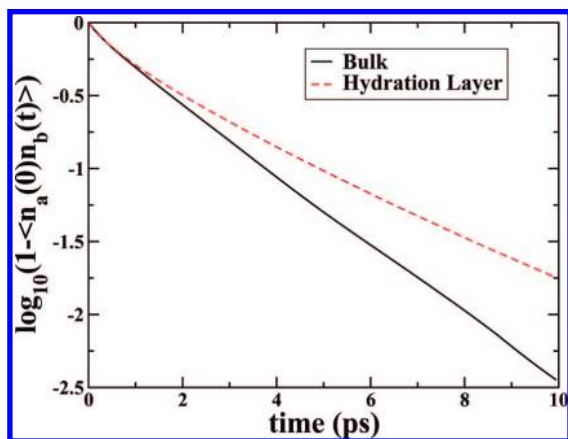


Figure 3. Decay of the WW H-bond correlation function in a semilog plot in bulk and hydration layer. The slope of this correlation function provides information about the H-bond switching rate. Note the slow decay of the correlation function in the hydration layer as compared to bulk water, indicating a slower switching rate in the hydration layer.

otherwise, and n_b is 1 when H* is hydrogen-bonded to Oⁿ and 0 otherwise.¹⁶ We have neglected the transient breaking of the bond. In addition, the absorbing boundary conditions are used for n_b so that when a particular hydrogen bond has broken, it never reforms. We thus discard the contribution from back-reaction, and the rate constant extracted from these correlation functions will give the forward rate of hydrogen bond switching. Figure 3 shows the decay of the correlation function for the hydration layer and bulk water in a semilog plot. Decay of the hydrogen bond lifetime correlation function in the bulk water is monoexponential with the characteristic time constant $\tau_0 = 1.8$ ps. This is in agreement with earlier simulation studies.¹⁶ The characteristic time constant of the correlation function obtained in the hydration layer is $\tau_0 = 2.6$ ps. The jump frequency parameter, $1/\tau_0$, corresponds to the rate constant of the HBSE. Note that this hydrogen bond lifetime correlation function calculated for the forward rate of breaking is not equal to $C(t)$, usually calculated for H-bond lifetime,^{26–28} but rather like $S(t)$ without the transient bond breaking. We have also observed that the re-formation of the H-bond with the old acceptor is more frequent in the hydration layer, which makes the H-bond dynamics even slower. Note that the estimate of 2.6 ps includes the average over all HBSEs (BDHB and FDHB) in the hydration layer. We find that the forward rate of H-bond breaking is much slower (about 3–4 times) for BDHB than for FDHB.

(C) Longevity of HB Network. We now discuss the longevity of the H-bond network in the hydration layer of lysozyme. Earlier studies have shown that the network is more stable near a hydrophilic residue than near a hydrophobic one.^{14,15} We have also explored the H-bond network longevity around hydrophilic and hydrophobic residues through the rate of H-bond breaking. Figure 4a and b show the spectrum of partner change of H-bond for water molecules that are hydrogen-bonded to a hydrophilic amino acid (BDHB) and are around hydrophobic residues (FDHB), respectively. Note that the partner change is much less frequent for the water molecules that are hydrogen-bonded to a hydrophilic residue (Figure 4a), indicating that the H-bond network is long-lived near the hydrophilic surface. The partner change is more frequent for the water molecule, which is not hydrogen-bonded to a protein and is around a hydrophobic residue (Figure 4b), indicating that the longevity of the H-bond network is shorter near a hydrophobic surface. The origin of this enhanced longevity of the

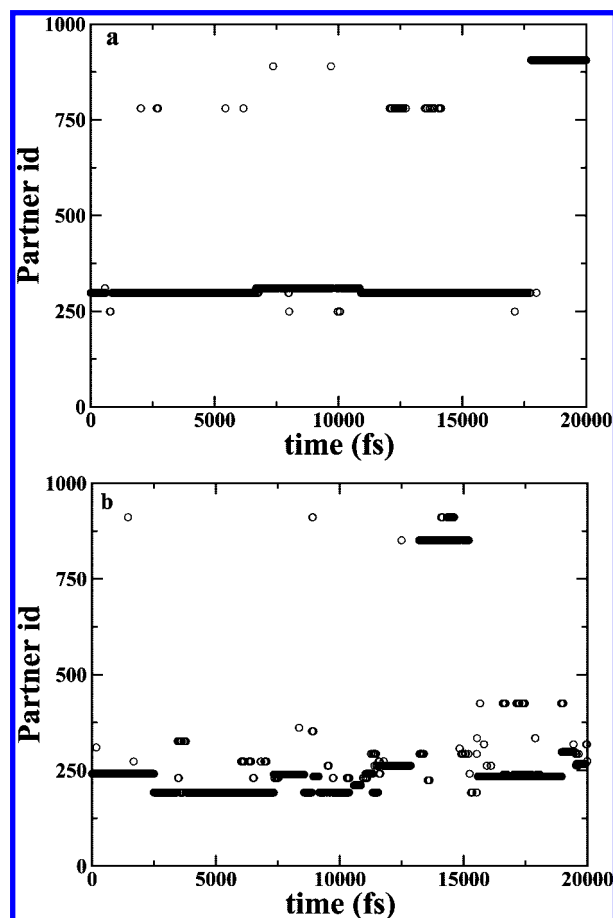


Figure 4. Spectrum of H-bond partner change of a donor water molecule of (a) BDHB (near a hydrophilic residue), and (b) FDHB (near a hydrophobic residue). The step along the Y-axis indicates the partner change. Note the less frequent partner change near the hydrophilic surface as compared to the hydrophobic surface.

H-bond network near a hydrophilic surface is the increased electrostatic interactions between the polar amino acid residues and the water molecules.

(D) Angular van Hove Self-Correlation Function. We now focus on the effect of translational–rotational coupling on the rotational dynamics of water molecules in the bulk and hydration layer. To this end, we have calculated an orientation analogue of the van Hove self-correlation function ($G(\theta, t)$), which is defined as

$$G(\theta, t) = \langle \delta[\theta_i - \theta_i(t)] \rangle, \quad (1)$$

where $\theta_i(t) = \cos^{-1}[u_i(0) \cdot u_i(t)]$ and u_i are the directions of the individual O–H bonds. Figure 5a and b displays the angle distribution $\sin \theta G(\theta, t)$ at three different times for bulk water and hydration layer water molecules, respectively. Although the distribution in the bulk water (Figure 5a) at longer times is smooth and homogeneous over the whole θ range, a two-peak character is evident in the hydration layer (Figure 5b).

In a recent study, it was observed that translational mobility of nitrate ions (NO_3^-) plays a critical role in the rotational motion of the same.²⁹ It has been observed that in the case of translationally mobile ions, the angle distribution at longer time is continuous over the whole θ range, indicating that mobile ions mostly perform small angle rotational diffusion, in addition to the large angle jump motion. On the other hand, a translationally immobile ion can perform only large-angle hopping, which induces a well-separated two-peak character to the angle distribution at longer times.²⁹

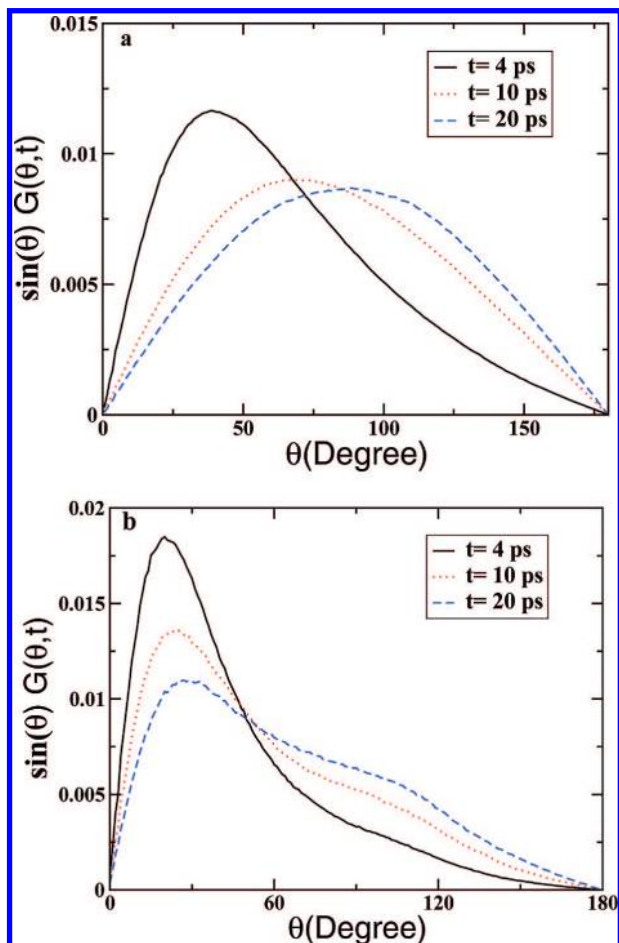


Figure 5. The angle distribution ($\sin \theta G(\theta, t)$) associated with the van Hove self-correlation function at three different times ($t = 4, 10,$ and 20 ps) in (a) bulk water and (b) hydration layer. Note the two-peak character of the distribution for hydration layer water at longer times.

The difference in the behavior of the angle distribution between the bulk and hydration layer water can thus be understood as follows: (i) Bulk water can perform angular jumps during HBSE, but diffusion of the center of mass is accompanied by small-angle rotational diffusion. (ii) During the time that hydration layer water is translationally constrained in a given location, small-angle rotational diffusion is suppressed as compared to bulk, but they are allowed to perform the hopping by large angles. We now provide further evidence of this coupling between translational and rotational motion.

(i) We have calculated the $G(\theta, t)$ of bulk water at a lower temperature (250 K), where the translational motion is sufficiently constrained, and found a strong two-peak character of the angular distribution ($\sin \theta G(\theta, t)$) emerges at longer times, as shown in Figure 6a.

(ii) We now present additional evidence of the translation–rotation coupling. To this end, we have selected two sets of water molecules near the protein surface: (1) water within the hydration layer (within 4.25 \AA of the protein surface) and (2) water within 3.5 \AA of the protein surface. We have calculated $G(\theta, t)$ for these two sets of water, and the angle distribution at longer time is displayed in Figure 6b. We have also plotted the angle distribution of bulk water in the same plot for comparison. Although the bulk water distribution is smooth and homogeneous, a two-peak character is evident for the hydration layer. This two-peak character of the angular distribution becomes more prominent for the water molecules within 3.5 \AA of the

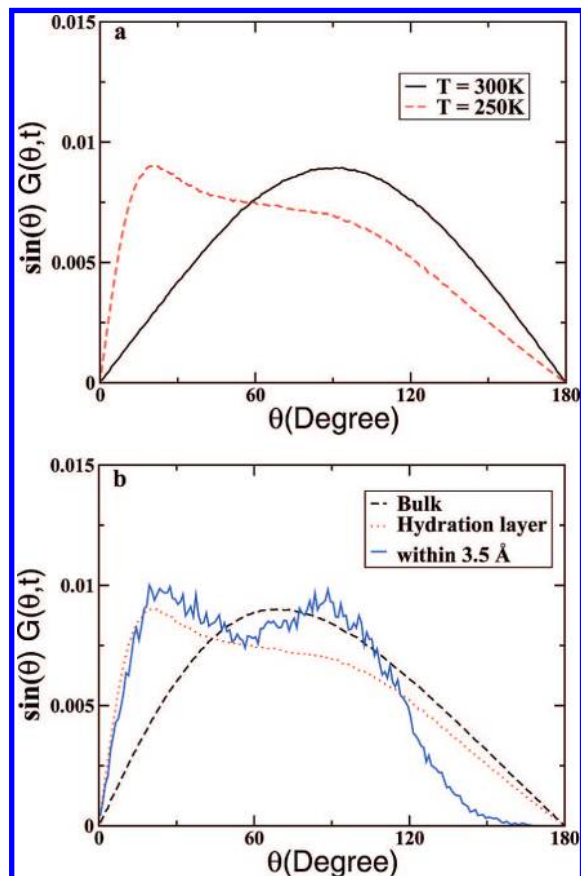


Figure 6. (a) The angle distribution ($\sin \theta G(\theta, t)$) associated with the van Hove self-correlation function at long time in the bulk water at 300 and 250 K. Note the two-peak character of the distribution for 250 K. (b) The angle distribution ($\sin \theta G(\theta, t)$) associated with the van Hove self-correlation function at long time in the bulk water, hydration layer, and layer within 3.5 \AA from the protein surface at 300 K. Note the presence of the two-peak character in the distribution for the hydration layer and the layer within 3.5 \AA . The two-peak character is more prominent for the latter.

protein surface. Water molecules that stay within 3.5 \AA of the protein surface for long time are found to be H-bonded to the protein. These water molecules are translationally more constrained and, hence, less mobile than those of the hydration layer (within 4.25 \AA of the protein surface), which are in turn more immobile than the bulk water. Therefore, when the motion of the water molecule is translationally immobile, the rotational motion of water molecules occurs through large amplitude jumps.

IV. Conclusions

We have discovered three different bond-breaking and reorientation mechanisms in the hydration layer that are different from that in the bulk water. A large angle jump of the direction of the rotating O^*-H^* bond is found to be common for all the reorientation processes. From a comparison of the mechanisms between the hydration layer and bulk, we conclude that the translationally constrained hydration layer sustains a connected hydrogen bond network that is responsible for the unusual dynamical behavior. We have discussed the mechanism of HB breaking, forward rate of HB breaking, and longevity of the HB network in terms of the topological disorder of the surface of protein. We have explored the effect of translational–rotational coupling on the rotational motion of water molecules through

the angular van Hove self-correlation function, which shows the evolution of a two-peak structure in the layer that is absent in the bulk.

Acknowledgment. This work has been supported in part by grants from DST and JC Bose Fellowship, India. B.J. and S.P. acknowledge CSIR, India for providing a research fellowship. We thank Dr. Swapan Roychowdhury and Mr. Bharat V. Adkar for helpful discussions.

References and Notes

- (1) Levy, V.; Onuchic, J. N. *Annu. Rev. Biophys. Biomol. Struct.* **2006**, *35*, 389.
- (2) Raschke, T. M. *Curr. Opin. Struct. Biol.* **2006**, *16*, 152.
- (3) Bhattacharyya, K.; Bagchi, B. *J. Phys. Chem. A* **2000**, *104*, 10603.
- (4) Bagchi, B. *Chem. Rev.* **2005**, *105*, 3197.
- (5) Daniel, R. M.; Finney, J. L.; Stoneham, M. *Philos. Trans. R. Soc. London, Ser. B* **2004**, *359*, 1143.
- (6) Timasheff, S. N. *Annu. Rev. Biophys. Biomol. Struct.* **1993**, *22*, 67.
- (7) Nandi, N.; Bagchi, B. *J. Phys. Chem. B* **1997**, *101*, 10954; *J. Phys. Chem. A* **1998**, *102*, 8217.
- (8) Stanley, H. E.; Kumar, P.; Xu, L.; Yan, Z.; Mazza, M. G.; Buldyrev, S. V.; Chen, S.-H.; Mallamace, F. *Physica A* **2007**, *386*, 729.
- (9) Ohmine, I.; Tanaka, H. *Chem. Rev.* **1993**, *93*, 2545.
- (10) Jordanides, X. J.; Lang, M. J.; Song, X.; Fleming, G. R. *J. Phys. Chem. B* **1999**, *103*, 7995.
- (11) Murarka, R. K.; Head-Gordon, T. *J. Phys. Chem. B* **2008**, *112*, 179.
- (12) Pizzitutti, F.; Marchi, M.; Sterpone, F.; Rossky, P. J. *J. Phys. Chem. B* **2007**, *111*, 7584.
- (13) Li, T.; Hassanali, A. A.; Kao, Y.-T.; Zhong, D.; Singer, S. J. *J. Am. Chem. Soc.* **2007**, *129*, 3376.
- (14) Khoshtariya, D. E.; Hansen, E.; Leecharoen, R.; Walker, G. C. *J. Mol. Liq.* **2003**, *105*, 13.
- (15) Yokomizo, T.; Higo, J.; Nakasako, M. *Chem. Phys. Lett.* **2005**, *410*, 31.
- (16) Laage, D.; Hynes, J. T. *Science* **2006**, *311*, 832.
- (17) Laage, D.; Hynes, J. T. *Proc. Natl. Acad. Sci. U.S.A.* **2007**, *104*, 11167.
- (18) Laage, D.; Hynes, J. T. *Chem. Phys. Lett.* **2006**, *433*, 80.
- (19) Sciortino, F.; Geiger, A.; Stanley, H. E. *Nature (London)* **1991**, *354*, 218.
- (20) van der Spoel, D.; Lindahl, E.; Hess, B.; van Buuren, A. R.; Apol, E.; Meulenhoff, P. J.; Tieleman, D. P.; Sijbers, A. L. T. M.; Feenstra, K. A.; van Drunen, R.; Berendsen, H. J. C. *Gromacs User Manual*, version 3.2, 2004 www.gromacs.org.
- (21) Berendsen, H. J. C.; Grigera, J. R.; Straatsma, T. P. *J. Chem. Phys.* **1987**, *91*, 6269.
- (22) (a) Darden, T.; York, D.; Pedersen, L. *J. Chem. Phys.* **1993**, *98*, 10089. (b) Essmann, U.; Perera, L.; Berkowitz, M. L.; Darden, T.; Lee, H.; Pedersen, L. G. *J. Chem. Phys.* **1995**, *103*, 8577.
- (23) Rey, R.; Møller, K. B.; Hynes, J. T. *J. Phys. Chem. A* **2002**, *106*, 11993.
- (24) Lawrence, C. P.; Skinner, J. L. *J. Chem. Phys.* **2003**, *118*, 264.
- (25) Eaves, J. D.; Loparo, J. J.; Fecko, C. J.; Roberts, S. T.; Tokmakoff, A.; Geissler, P. L. *Proc. Natl. Acad. Sci. U.S.A.* **2005**, *10*, 13019.
- (26) Luzar, A.; Chandler, D. *Nature* **1996**, *379*, 55.
- (27) Luzar, A.; Chandler, D. *Phys. Rev. Lett.* **1996**, *76*, 928.
- (28) Chandra, A. *Phys. Rev. Lett.* **2000**, *85*, 768.
- (29) Rebeiro, C. C. M. *Phys. Chem. Chem. Phys.* **2004**, *6*, 771.

JP800998W